Newcastle University

ePrints

Kassotakis N, Sarhosis V, Forgács T, Bagi K.

Discrete element modelling of multi-ring brickwork masonry arches.

***In: 13th Canadian Masonry Symposium*. 2017, Halifax, Canada: Canada Masonry Design Centre.**

Copyright:

This is the author's manuscript of a paper that was presented at 13th Canadian Masonry Symposium, held 4-7th June 2017, Halifax, Canada.

Copyright © 2017 Proceedings of the Thirteenth Canadian Masonry Symposium. Reprints of all or parts of these Proceedings and the Abstracts of the papers may be made on the condition that credit is given to the authors and reference is made to the Proceedings of the Thirteenth Canadian Masonry Symposium.

Link to conference website:

http://www.13thcms.com/

Date deposited:

04/04/2017

Newcastle University ePrints - eprint.ncl.ac.uk

13TH CANADIAN MASONRY SYMPOSIUM
HALIFAX, CANADA
JUNE 4TH – JUNE 7TH 2017

DISCRETE ELEMENT MODELLING OF MULTI-RING BRICKWORK MASONRY ARCHES

Kassotakis, Nicko[1]; Sarhosis, Vasilis[2]; Forgács, Tamás[3] and Bagi, Katalin[4]

ABSTRACT

A significant portion of the UK's bridge stock is represented by multi-ring brickwork masonry arches. Most of these bridges are well over 100 years old and are supporting traffic loads many times above those originally envisaged. Different materials and methods of construction used in these bridges will influence their strength and stiffness. There is an increasing demand for a better understanding of the life expectancy of such bridges in order to inform repair, maintenance and strengthening strategies. This paper presents the first development of a three dimensional computational model, based on the Discrete Element Method (DEM), which was used to investigate the load carrying capacity and failure mechanism of multi-ring masonry arch bridges. Each brick of the arch was represented as a distinct block jointed by zero thickness interfaces. In this way, complete block separation and large movements of the masonry blocks are allowed. First the suitability of DEM to accurately predict the load carrying capacity and failure mode is investigated by comparing the numerical results against those obtained from experimental studies. Then, a parametric analysis carried out to understand the influence of the: a) number of rings; b) arch span; and c) rise to span ratio on the load carrying capacity and failure mode of multi-ring arches. From the results analysis, it was found that DEM is a capable approach to simulate the mechanical behaviour of multi-ring arches. From the parametric study, it was found that all arches failed by the formation of a four-hinge mechanism. Also, as the number of arch rings' increases, the load carrying capacity of the arches increases proportionally.

KEYWORDS: *Arches*, *Brickwork*, *DEM, Masonry, Multi-ring*

[1] PhD student, School of Civil Engineering and Geosciences, Newcastle University, Newcastle upon Tyne, UK, n.kassotakis2@newcastle.ac.uk
[2] Assistant Professor, School of Civil Engineering and Geosciences, Newcastle University, Newcastle upon Tyne, UK, vasilis.sarhosis@newcastle.ac.uk
[3] PhD student, Department of Structural Mechanics, Budapest University of Technology and Economics, Hungary, tamasforgacs@hotmail.com
[4] Professor, Department of Structural Mechanics, Budapest University of Technology and Economics, Hungary, kbagi@mail.bme.hu

1. INTRODUCTION

There are thousands of multi-ring brickwork masonry arch bridges in the UK. Most of these bridges were built over a century ago and support traffic loads much higher than those originally designed to carry. Fatigue, deterioration of materials and changing load regimes create an increasing demand for a better understanding of their current structural condition and long term behaviour in order to inform appropriate repair, maintenance and rehabilitation strategies [1]. To date, extensive experimental work has been carried out to study the ultimate limit state behaviour and failure mode of plain and strengthened multi-ring brickwork arches [2, 3, 4]. From such studies, it was observed that multi-ring brickwork arches have inherently different performance characteristics to those of voussoir arches. This is because the mortar joints between rings (which are weak in tension and shear) can form potential planes of weakness which could have serious consequences with regard to their long term behaviour and load carrying capacity [5]. Furthermore, numerical approaches such as the Rigid Block Analysis Method [6] and the Finite Element Method (FEM) have been used to numerically assess multi-ring arches [7]. FEM was used to predict shear capacities of mortar joints deemed critical when assessing ring separation [6, 8]. However, the main disadvantages of the FEM included: (a) high computational cost; and (b) convergence difficulties if blocks fall or slide excessively [1]. The Discrete Element Method (DEM) provides an alternative approach allowing the discrete nature of the masonry to be recreated [9]. Within DEM, the multi-ring brickwork masonry arch is considered as a collection of blocks/bricks able to move and rotate around each other. The DEM was initially developed by Cundall [10] to simulate rock sliding while later it has been applied to simulate blocky masonry structures, including old and deteriorated masonry arches [11, 12], where failure occurs along the mortar joints.

The aim of this paper is to investigate the influence of the number of rings, the arch span, and the rise to span ratio on the load carrying capacity and failure mechanism of multi-ring brickwork masonry arches. Due to the intention of this investigation being the effect of the arch ring geometry, the influence of fill has not been included. Among others, the final goal of this research is to provide further insight into the ultimate limit state behavior of multi-ring masonry arches.

2. OVERVIEW OF 3DEC FOR MODELLING MASONRY

3DEC is a computational software used to simulate the static and dynamic behavior of blocky structures and is based on the Discrete Element Method (DEM) of analysis. For masonry, blocks (i.e. bricks) are represented as rigid or deformable blocks, which may form any arbitrary geometry. For masonry structures with stiff components, rigid blocks are adequate as the strong units mean deformational behavior takes place at the joints. In the analyses reported herein, deformable blocks with an internal tetrahedral uniform-strain FE mesh were used. Mortar joints were represented by zero thickness interfaces and governed by appropriate stress-displacement constitutive laws which can be viewed as interactions between the blocks. Contacts are of either vertex to face or edge-to-edge type (Fig. 1). Finite displacements of the discrete bodies and rotations are allowed. This includes complete detachment of blocks and new contact generation as the calculation proceeds. Contacts can open and close from the application of the external load depending on the stresses

acting on them. Forces in shear and normal direction are considered linear functions of the actual penetration in shear and normal directions respectively [13]. The mechanical behavior of joints is governed by the following equation in the normal direction

$$\Delta\sigma_n = -JK_n \times \Delta U_n \tag{1}$$

in which JK_n is the normal stiffness of the contact, $\Delta\sigma_n$ the increment in normal stress and ΔU_n is the change in normal displacement during the actual last time step. Similarly, in the shear direction the mechanical behavior of mortar joints is controlled by constant shear stiffness JK_s using the following expression:

$$\Delta\tau_s = -JK_s \times \Delta U_s \tag{2}$$

in which $\Delta\tau_s$ is the increment in shear stress and ΔU_s is the change in shear displacement. These stress increments are added to the already accumulated stresses, and then the total normal and shear stresses are updated to meet the selected non-elastic failure criteria, such as the Mohr–Coulomb model. For all contacts, calculations are made using the force–displacement law and the Newton's second law of motion for all blocks. From known displacements, the force–displacement law is used to find contact forces. Newton's second law governs the motion of the blocks resulting from the known forces acting on them.

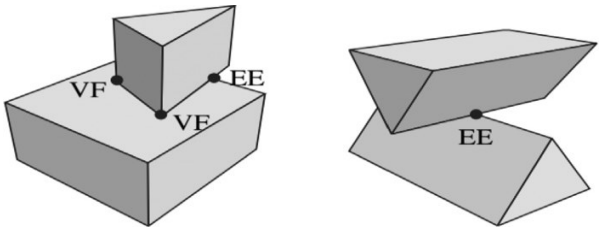

Fig. 1 Representation of Block interaction by elementary vertex-face (VF) and edge to edge (EE) point contacts in 3DEC ([13]).

3. COMPUTATIONAL MODELLING OF MASONRY ARCHES WITH 3DEC

3.1. Development of geometry and material parameters

Twenty-four different geometries of multi-ring arches were created in 3DEC (Table 1). The width of all arches was kept constant and equal to 0.48 m. All bricks were equal in size with dimensions (215 mm x 102.5 mm x 65 mm). To accommodate varying curvature of rings, blocks in 3DEC were constructed having a pentagonal prism shape (Fig 2). The ring thickness was 0.1025 m in every case. For normal spans, block shape tended to a rectangular cuboid. Mortar joints were assumed to behave in an elasto-plastic relationship with residual strength [13]. Both tension and cohesion resistance were taken into consideration. Material parameters for the masonry bricks and the mortar joints used in the analyses were obtained from the literature [14, 15, 16, 17] and are shown in (Tables 2 and 3).

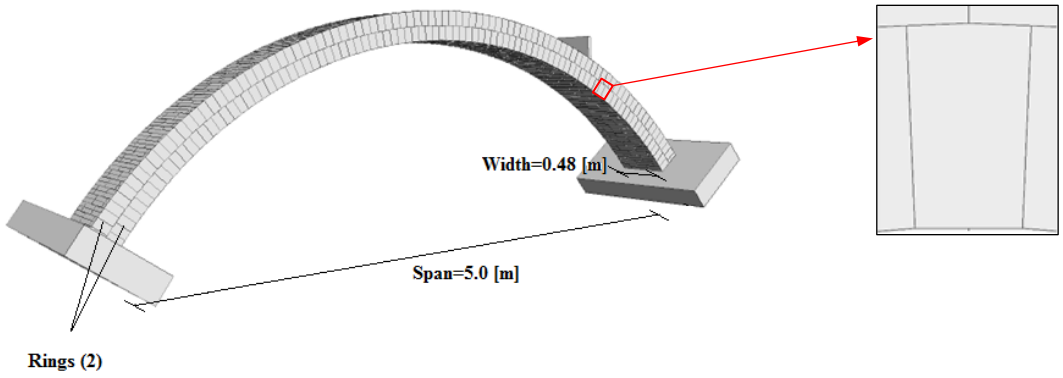

Fig. 2 Typical Geometry of a Two Ring Arch constructed in 3DEC (Arch Group B; ref. Table 1).

Table 1: Arch Dimensions Used in the Analysis.

Arch Group	Span [m]	Rise to Span Ratio	Number of Rings	Width [m]
A	3.0	1:4	2 to 5	0.475
B	5.0	1:4	2 to 5	0.475
C	7.0	1:4	2 to 5	0.475
D	9.0	1:4	2 to 5	0.475
E	5.0	1:3	2 to 5	0.475
F	5.0	1:2	2 to 5	0.475

Table 2: Properties of Masonry Units.

Density [kg/m^3]	Young's Modulus [N/m^2]	Poisson's Ratio [-]	Bulk Modulus [N/m^2]	Shear Modulus [N/m^2]
2,368	33.85E9	0.19	18.2E9	14.2E9

Table 3: Properties of Interfaces.

Joint Normal Stiffness [N/m^3]	Joint Shear Stiffness [N/m^3]	Joint Friction Angle [Degrees]	Joint Tensile Strength [N/m^2]	Joint Cohesive Strength [N/m^2]	Joint Dilation Angle Modulus [Degrees]
20E9	15E9	30	0.06E6	0.06 E6	0

3.2. Boundary conditions and loading

The abutments of the arch were modelled as rigid supports, both in vertical and horizontal directions. A gravitational load was assigned for self-weight effects. The model was initially

brought into equilibrium under its own self-weight. A full width line load was applied incrementally at the quarter span of the arch. The loading history imposed by applying a velocity equal to 0.003 m/s at the loading block and the evolution of the displacement recorded. The zero thickness interface between the loading platen and the extrados of the arch was made stiffer (e.g. friction angle set to 90 degrees). In this way, no slippage of the loading platen took place during loading.

3.3. Validation of the computational model/ Representative Results Load-Displacement Graph

The reliability of the numerical model was evaluated by comparing the a) experimental against the predicted by the numerical analysis failure modes (Fig. 3); and b) the load-displacement graph obtained from 3DEC simulations against those from the experiment (Fig.4) [14]. From Figs. 3 & 4, good correlation was obtained between the experimental and the numerical results.

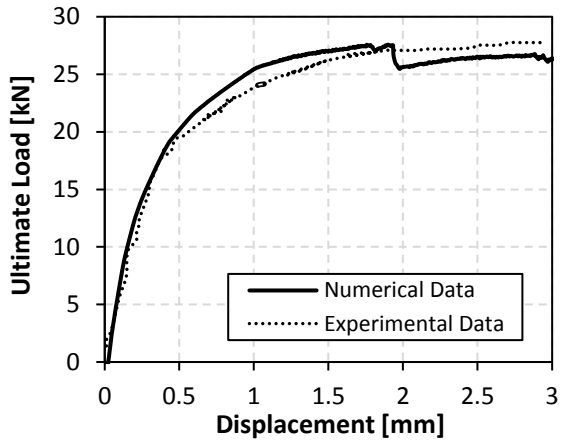

Fig. 3. Comparison of Experimental Against Numerical Load vs. Displacement Curves [14]

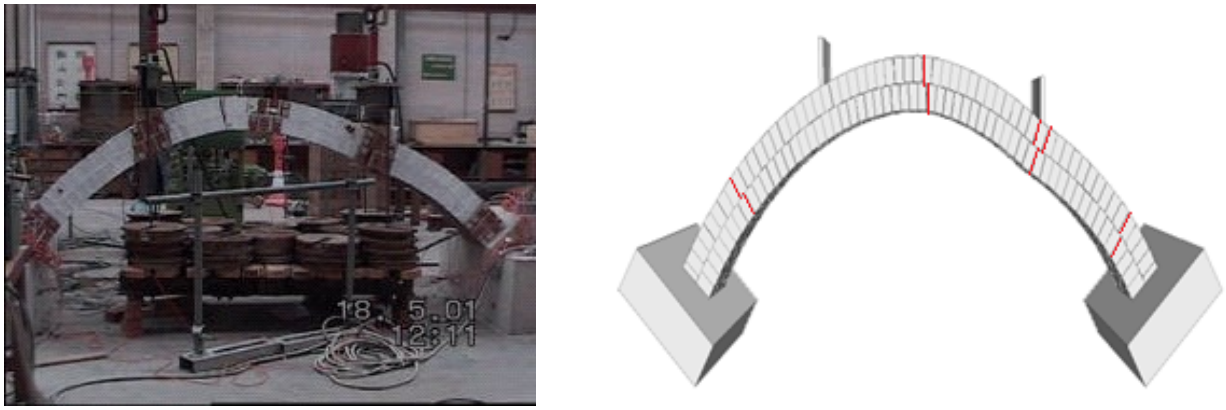

a.) Experimental failure mode **b.) Numerical failure mode**

Fig. 4. Failure modes observed during the: (a) Experimental test [14]; (b) Numerical analysis (note: red thick lines indicate major cracks in the arch)

4. PARAMETRIC ANALYSIS

4.1. Influence of the number of rings, rise:span ratio and arch span on the ultimate load carrying capacity of the arches

Figs. 5a and 5b show the ultimate load carrying capacity of multi-ring arches studied numerically. The ultimate load carrying capacity of arches increases almost linearly as the number of rings increases. Also, for a given span and the same number of rings, the ultimate load carrying capacity of arches increases as the rise to span ratio decreases (e.g. segmental arches can carry more load than the circular ones; having the same thickness. For example, for an arch having a span of 5 m and five rings, the difference in ultimate load carrying capacity between 1:4 and 1:2 rise:span was found to be 54%. The ultimate load carrying capacity of arches decreases as the span length grows for a constant rise:span ratio equal to 1:4. For example, the increase in the ultimate load carrying capacity of 3 m span arches with 2 and 3 rings was found to be 108%.

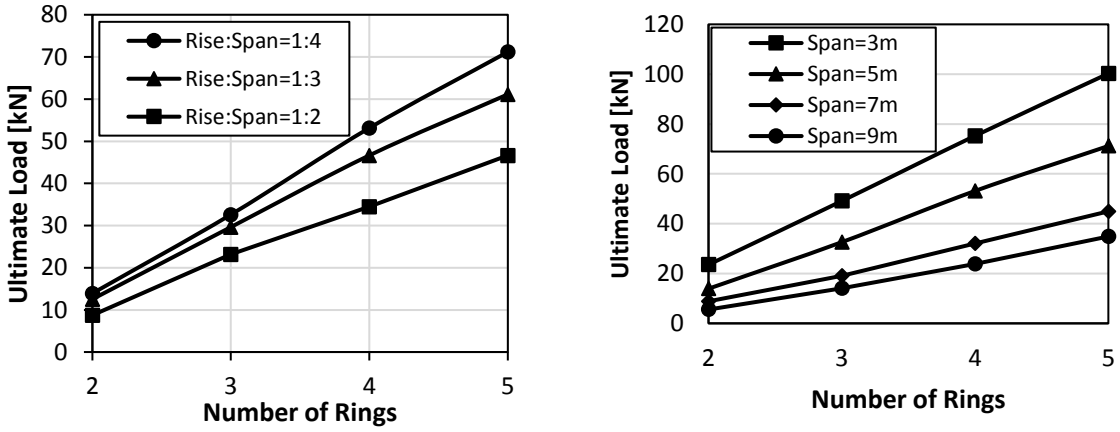

a.) Span is 5 m **b.) Rise:Span is 1:4**

Fig. 5. Ultimate load against number of rings for the different arches studied numerically.

4.2. Influence of the number of rings upon failure mode of the arch

The failure modes for differing rise:span ratio and span lengths are presented in Fig. 6. In all cases, the four-hinge failure mechanism was observed. For arches having smaller number of rings, the crack formation was more distinguishable, expressing less defused hinge formations. For arches having larger numbers rings, hinges were more defused having multiple radial cracks which spread with the application of load until the failure. Ring separation was not found to occur.

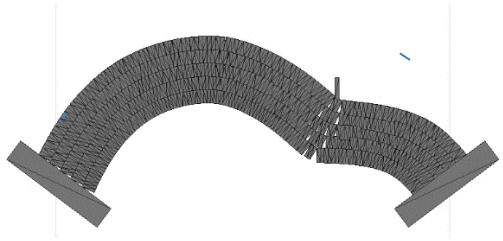

a.) Span 3 m, rise:span 1:4, rings 2

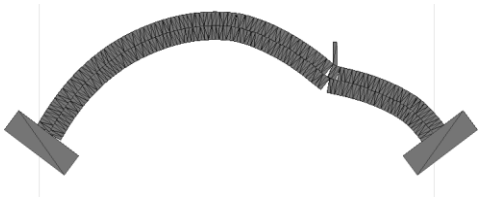

b.) Span 3 m, rise:span 1:4, rings 5

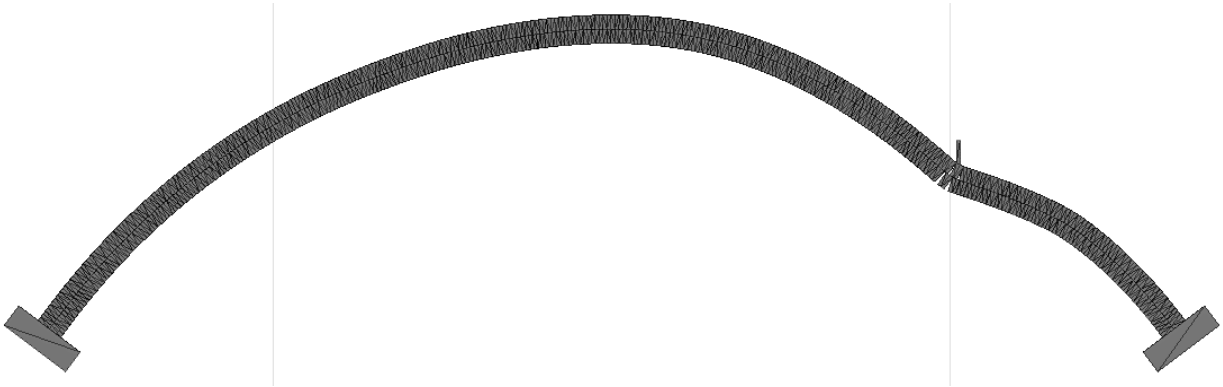

c.) Span 9 m, rise:span 1:4, rings 2

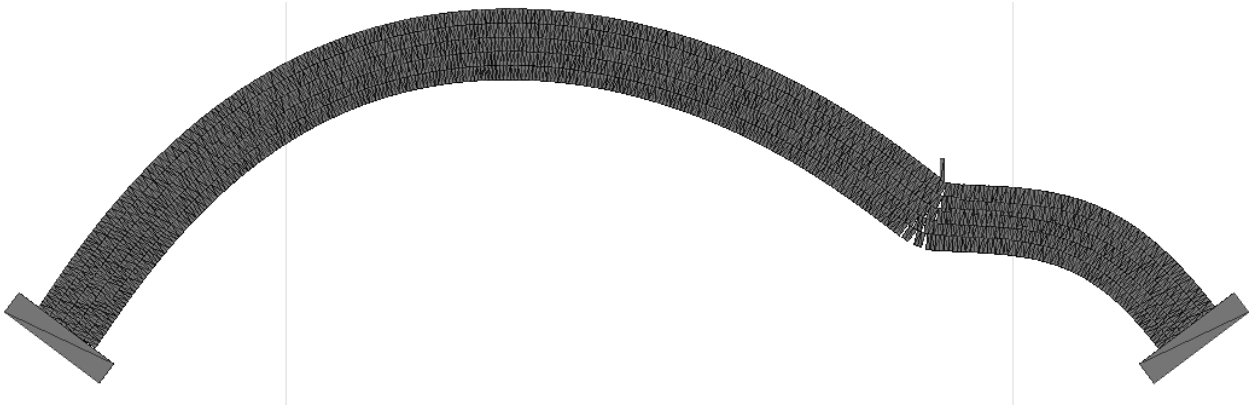

d.) Span 9 m, rise:span 1:4, rings 5

Fig. 6. Failure modes obtained from the numerical model (not to scale)

The accompanying principal forces in the arch for loads approaching failure are shown in Fig. 7. The extremities, being red and blue color express the zones of failure and cracking. The red zones denotes tensile forces whereas the blue demonstrate compressive forces. Stresses in the five and two ring arches were in the region of -7 to 1.2 MPa and -3 to 0.6 MPa accordingly**.**

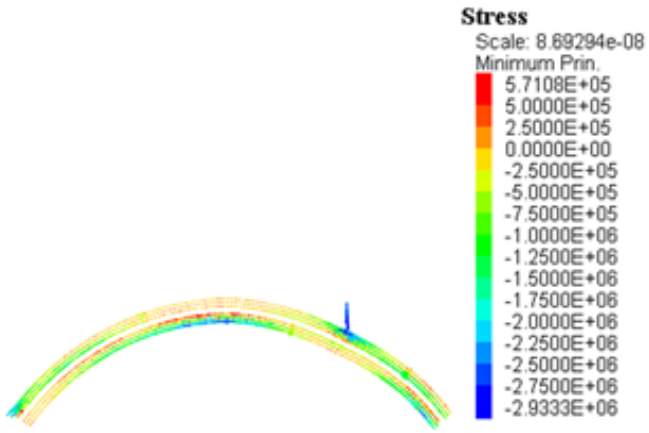

a.) Span 3 m, rise:span 1:4, rings 2

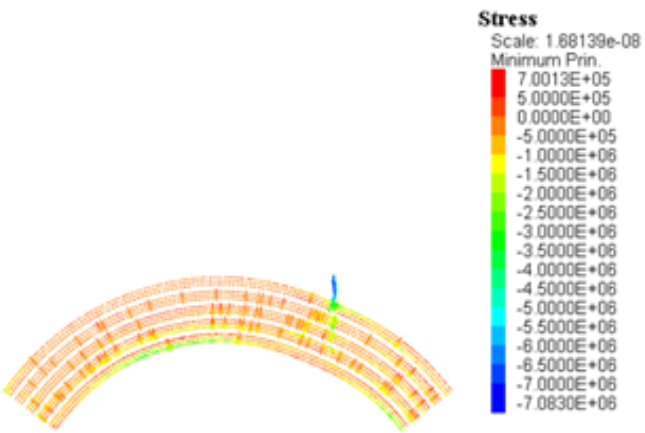

b.) Span 3 m, rise:span 1:4, rings 5

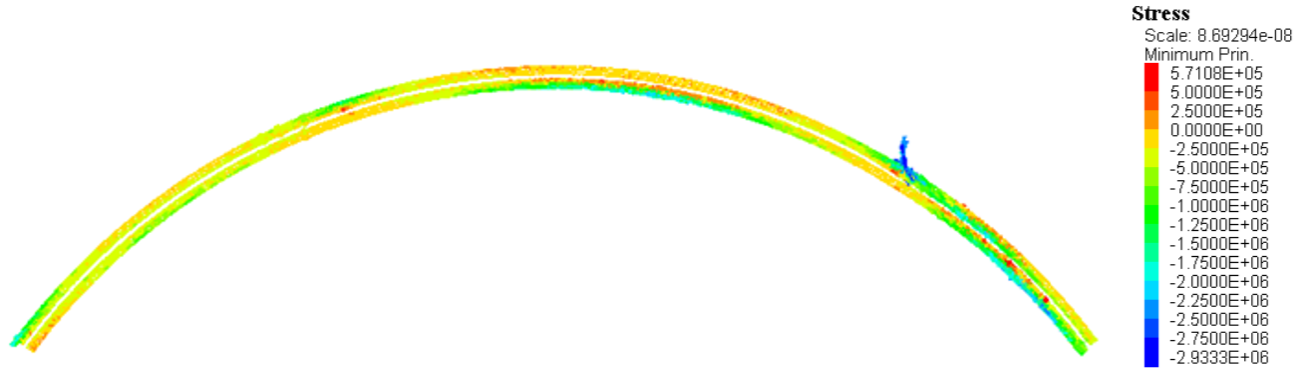

c.) Span 9 m, rise:span 1:4, rings 2

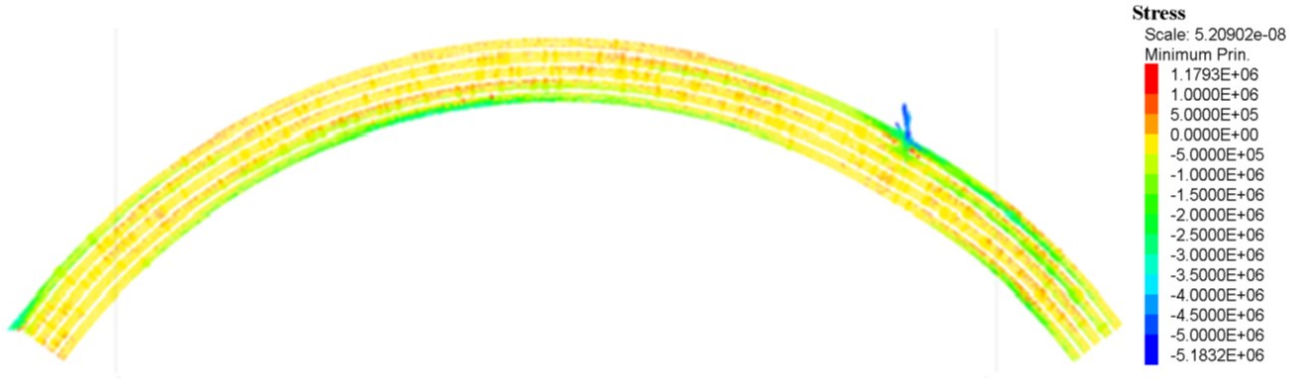

d.) Span 9 m, rise:span 1:4, rings 5

Fig. 7. Principal stresses at the arch (not to scale)

4.3. Influence of the number of rings upon stiffness of the arch with different span and rise:span ratios

The tangent of the load-displacement curve below in Fig. 8 shows an estimate of arch stiffness before cracking occurs. Specifically the tangent of each load-displacement curve describes the stiffness of each arch. Arch stiffness increases as the ring number increases. The increase of stiffness is larger for lower ring number additions. In certain the most significant increase in stiffness for addition of ring number was most for shorter spanned arches. Specifically, 3 m span arches of 2 rings and 3 ring had a difference in stiffness of 111%.

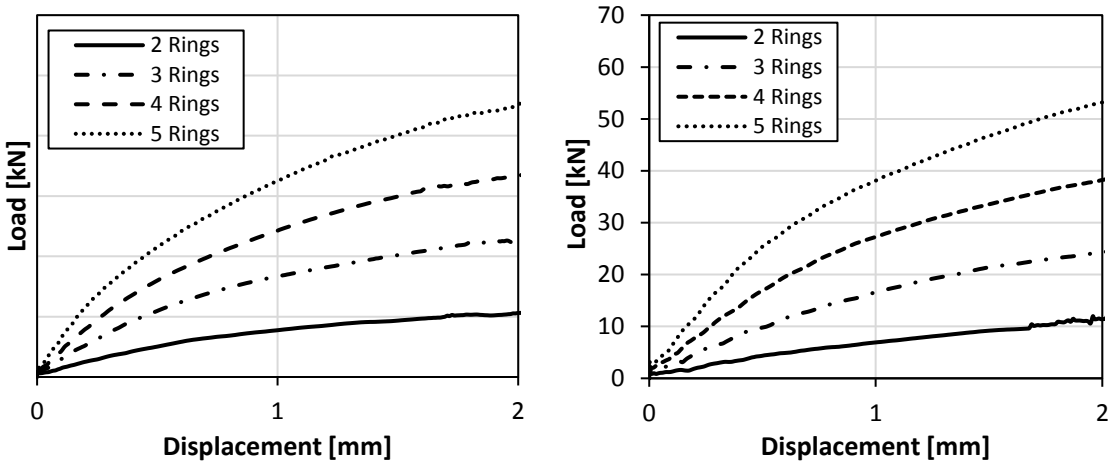

(a) Span = 3 m. **(b) Span = 5 m.**

Fig. 8. Load against quarter span vertical displacement curves for rise to span ratio of 1:4 m and differing span length

5. CONCLUSIONS

The Discrete Element Method in the form of the 3DEC software has been used to investigate the effect of the number of rings on the load carrying capacity of twenty four single span multi-ring brick masonry arches. A full width linear increasing load was applied to the extrados of each arch at the quarter span until structural failure was reached. The joints had non-zero tension resistance and cohesion. The mode of failure and ultimate load that each arch could carry due to application of load were recorded. The main conclusions of this study are: (a) 3DEC was capable of depicting the evolution of load with the progressive hinge development; (b) each arch barrel failed by the development of a four-hinge mechanism and no ring separation occurred; (c) for arches having the same span, their ultimate load carrying capacity proportionally increases as the number of rings increases; (d) for arches having smaller number of rings, the crack formation was more distinguishable, expressing less defused hinge formations; (e) for arches having larger numbers of rings, hinges were more defused having multiple radial cracks which spread with the application

of load until failure; (f) for lower rise:span ratio and short spanned arches, the ultimate load bearing capacity was more dependent upon the ring number.

ACKNOWLEDGEMENTS

The work presented in this paper is financially supported by the EPSRC Comparative Award in Science and Engineering (CASE/179/65/82) and OTKA 100770 grant.

REFERENCES

[1] Sarhosis V, De Santis S, de Felice G. (2016). "A review of experimental investigations and assessment methods for masonry arch bridges. Structure and Infrastructure Engineering." *J. Mechanics Research Communications*, 12 2016 1439-1464.

[2] Garrity S. W. (2010). "Repair and strengthening of five full scale masonry arch bridges." *Proc. of 8th International Conference on Short and Medium Span Bridges,* Canada 2010.

[3] Melbourne C. Adrienn K. Tomor (2004). "Fatigue Performance of Composite and Radial-Pin Reinforcement on Multi-Ring Masonry Arches." *Proc., 4th International Conference of Arch Bridges ARCH´04,* CIMNE, Barcelona.

[4] Sumon, S.K. (1998). "Repair and strengthening of five full scale masonry arch bridges." *Proc. 2nd International Conference on Arch Bridges Venice,* pp. 379-381.

[5] Melbourne C, Gilbert M (1995). "The behaviour of multi-ring brickwork arch bridges. *Structural Engineers International Journal."* Institution of Structural Engineers 73:39–47.

[6] Gilbert, M (1998). "On the analysis of multi-ring brickwork arch bridges." *Proc. 2nd International Arch Bridges Conference, Venice,* pp. 109-118.

[7] Tao, Y, Chen, J-F, Stratford, T & Ooi, J (2012). "Numerical Modelling of a Large Scale Model Masonry Arch Bridge." Paper presented at Structural Faults and Repair 2012, Edinburgh, UK.

[8] Zhang Y. et al (2016). "Mesoscale partitioned analysis of brick-masonry arches." *J. Engineering Structures*, 61 (2014) 53–59.

[9] Sarhosis V, Bagi K, Lemos JV, Milani G. (2016). *Computational modelling of masonry structures using the discrete element method,* USA: IGI Global.

[10] Cundall, P.A., (1971). "A computer model for simulating progressive large scale movements in blocky rock systems." *International Society of Rock Mechanics; Proc. Intern. Symp., Nancy, France.*

[11] Lemos, J.V., (1995). *Assessment of the ultimate load of a masonry arch using discrete elements. In: Middleton*, J., Pande, G.N. (Eds.), Computer Methods in Structural Masonry – 3. Books & Journals International, Swansea, UK.

[12] Sarhosis V. et al (2014). "The effect of skew angle on the mechanical behavior of masonry arches." *J. Mechanics Research Communications*, 61 (2014) 53–59.

[13] Itasca (2004). *Universal Distinct Element Code Manual. Theory and Background,* Itasca Consulting Group, Minneapolis.

[14] Melbourne, C., Hodgson, (2004). "Cyclic load capacity and endurance limit of multi-ring masonry arches." *Proc., 4th International Conference of Arch Bridges ARCH´04,* Barcelona.

[15] Sarhosis V, Sheng Y (2014). "Identification of material parameters for low bond strength masonry." *Engineering Structures*, 60, 100-110.

[16] Van der Pluijm R. (1999). *Out-of-plane bending of masonry: behaviour and strength,* Eindhoven: Technische Universiteit Eindhoven.

[17] Zhang Y. 2015. *Advanced nonlinear analysis of masonry arch bridges*, PhD thesis, Imperial College London, London.